Development of a Model for the δ Opioid Receptor Pharmacophore. 1. Conformationally Restricted Tyr[1] Replacements in the Cyclic δ Receptor Selective Tetrapeptide Tyr-c[D-Cys-Phe-D-Pen]OH (JOM-13)†

Henry I. Mosberg,* Andrei L. Lomize, Chenguang Wang, Heather Kroona,‡ Deborah L. Heyl,§ Katarzyna Sobczyk-Kojiro, Wenli Ma, Carol Mousigian, and Frank Porreca||

College of Pharmacy, University of Michigan, Ann Arbor, Michigan 48109-1065, and Department of Pharmacology, University of Arizona, Tucson, Arizona 85719

Received September 28, 1994®

A series of analogues of the conformationally restricted δ opioid receptor selective tetrapeptide Tyr-c[D-Cys-Phe-D-Pen]OH (JOM 13) was prepared in which the conformationally labile Tyr residue was replaced with several less flexible tyrosine analogues. Among these tyrosine analogues were the bicyclic structures 1,2,3,4,-tetrahydro-7-hydroxyisoquinoline-3-carboxylic acid (HO-Tic), 2-amino-6-hydroxytetralin-2-carboxylic acid (Hat), and 2-amino-5-hydroxyindan-2-carboxylic acid (Hai) in which rotations about the $C^{\alpha}-C^{\beta}$ and $C^{\beta}-C^{\gamma}$ bonds are restricted due to cyclization of the side chain to the backbone. Also examined were analogues in which tyrosine was replaced with either *trans*-3-(4′-hydroxyphenyl)proline (*t*-Hpp) or *cis*-3-(4′-hydroxyphenyl)proline (*c*-Hpp), residues in which rotations about $C^{\alpha}-C^{\beta}$, but not $C^{\beta}-C^{\gamma}$, are restricted. Both the *t*-Hpp[1] and *c*-Hpp[1] analogues displayed δ receptor binding affinity similar to the parent Tyr[1]-containing peptide, while the D-Hat[1], L-Hat[1], and L-Hai[1] analogues exhibited somewhat lower affinity. The results observed for the *t*-Hpp[1] and *c*-Hpp[1] analogues are particularly significant since these two residues have little accessible conformational space in common. Since the binding conformation of residue 1 must be included in this limited conformational intersection, its elucidation is facilitated. Bioassay results from guinea pig ileum and mouse vas deferens preparations are in general agreement with the binding results; however some potency discrepancies are observed. These discrepancies may reflect different selectivities among δ receptor subtypes for the analogues or may represent differing efficacies among these conformationally restricted peptides. The conformational properties of the parent tetrapeptide and the residue 1-modified analogues were studied by molecular mechanics computations. All these peptides share a common rigid tripeptide cycle with a single energetically preferred backbone conformation and three different conformers of the D-Cys, D-Pen disulfide bridge, two of which are observed in the solid state and in aqueous solution, as previously determined from X-ray crystallography and ^{1}H NMR spectroscopy data (Lomize, A.; et al. *J. Am. Chem. Soc.* **1994**, *116*, 429–436). All the peptides have similar sets of low-energy conformations of their common flexible elements, the Phe[3] side chain and the peptide group between the first residue and the rigid tripeptide cycle. However, possible conformations of the first residue differ and depend on the covalent constraints incorporated into the side chain. Analysis of conformation–activity relationships obtained for these peptides allows the determination of some of the conformational requirements for their interaction with the δ opioid receptor. First, the side chain conformer of residue 1 in the δ receptor-bound state is determined to be *trans* ($\chi^1 \sim 180°$). Second, an extended conformation of the exocyclic peptide group (both ψ of residue 1 and φ of D-Cys[2] torsion angles are ~160°) is identified as providing the mutual arrangement of the first residue and the tripeptide cycle required for δ receptor binding.

Introduction

The incorporation of conformational constraints in analogues of biologically active peptides is a well-established approach for enhancing receptor selectivity and modulating efficacy, since, in principle, the resulting more rigid analogues may possess low-energy conformations suitable for interaction with one receptor type (or subtype) but not others or which may be appropriate for receptor recognition but not transduction.[1,2] In the opioid peptide area, conformational restriction *via* side chain to side chain cyclization, in particular, has been very effective, yielding highly selective δ[3,4] and μ[5] receptor agonists as well as highly selective μ receptor antagonists.[6] Employing this approach, we have developed three key analogues which display highly selective δ receptor agonist behavior: Tyr-c[D-Pen-Gly-Phe-D-Pen]OH (DPDPE, where Pen, penicillamine, is β,β-dimethylcysteine),[3] its L-Pen[5] diastereomer (DPLPE),[3] and the tetrapeptide Tyr-c[D-Cys-Phe-D-Pen]OH (JOM-13, **1**),[4] all of which are cyclized *via* a disulfide bond formed between side chain sulfhydryl groups. The incorporation of conformational constraints provides an added benefit since the resulting conformationally more

† Abbreviations and definitions recommended by IUPAC-IUB Commission of Biochemical Nomenclature have been used. Other abbreviations: α-MeTyr, α-methyl-Tyr; HO-Tic, 1,2,3,4,-tetrahydro-7-hydroxyisoquinoline-3-carboxylic acid; Hai, 6-hydroxy-2-aminoindan-2-carboxylic acid; Hat, 6-hydroxy-2-aminotetralin-2-carboxylic acid; c-Hpp and *t*-Hpp, *cis*- and *trans*-3-(4′-hydroxyphenyl)proline, respectively.

* To whom correspondence should be addressed.
‡ Present address: Cortech Inc., Denver, CO.
§ Present address: Department of Chemistry, Eastern Michigan University, Ypsilanti, MI 48197.
|| University of Arizona.

® Abstract published in *Advance ACS Abstracts*, November 1, 1994.

0022-2623/94/1837-4371$04.50/0

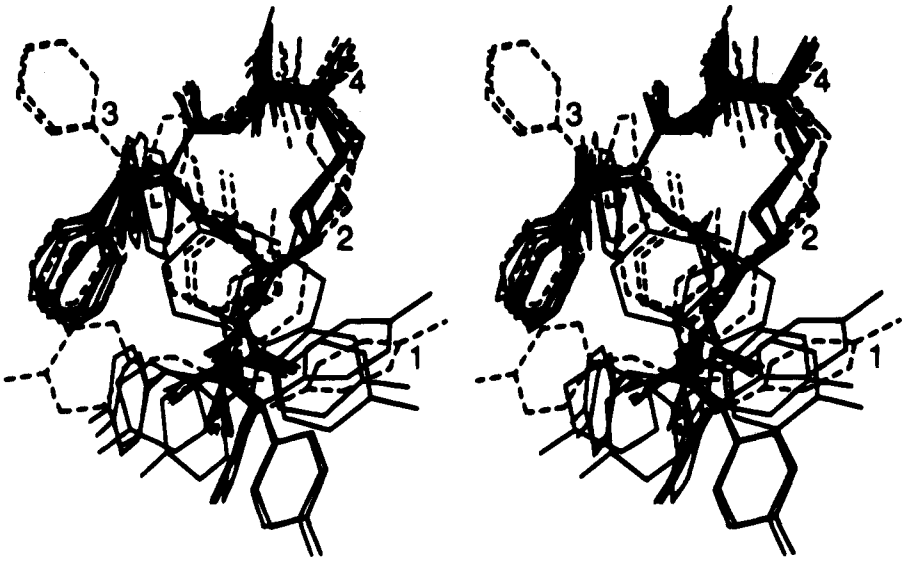

Figure 1. Superposition (stereoview) of 20 conformers of 1 with relative energies ΔE < 3 kcal/mol (QUANTA 3.3/CHARMm force field). Conformers with the χ^1 angle of Cys^2 ~ 180° are indicated by a dashed line. C^α atoms of the Tyr^1, D-Cys^2, and Phe^3 residues were used for superposition.

well-defined analogue serves as a better probe of the bioactive conformation at the specific receptor. This is because the more rigid analogue is less subject to the dynamic averaging that compromises attempts to elucidate the solution and bioactive conformations of the flexible, native peptide ligand. This can be seen in DPDPE, DPLPE, and **1** since in all cases the conformational flexibility of the backbone is considerably reduced by virtue of the cyclization. This is especially true of **1**, which was designed as a further contrained analogue of DPDPE, lacking the flexible central glycine residue of the pentapeptide.

We recently have reported the results of the conformational analysis of **1** employing solution NMR and solid state X-ray crystallographic experimental techniques as well as molecular mechanics calculations.[7] The peptide contains a rigid 11-membered cycle formed by its disulfide-containing C-terminal fragment, D-Cys-Phe-D-Pen. All low-energy conformers of **1**, with relative energies ΔE < 3.0 kcal/mol (Figure 1, Table 1), have very similar main chain torsion angles within the disulfide-containing cycle (the angles ψ of D-Cys^2, φ and ψ of Phe^3, and φ of D-Pen^4 in Table 1) but may be readily classified into three families, A, B, and C, which differ only in the geometry of the disulfide bridge (the χ^1, χ^2, and χ^3 angles of the D-Cys^2 and D-Pen^4 residues). The cyclic structures A and B are almost identical to independent conformers A_c and B_c of **1** in the unit cell revealed by X-ray crystallography and correspond to the two distinct ^{1}H NMR signal sets observed in aqueous solution.[7]

While the cyclic part of the molecule is conformationally well-defined, all the key elements of the opioid pharmacophore (exocyclic Tyr^1 residue and Phe^3 side chain) are still very flexible in solution. All *trans* (χ^1 ~ 180°), *gauche*$^+$ (χ^1 ~ −60°), and *gauche*$^-$ (χ^1 ~ 60°) rotamers of the Tyr^1 and Phe^3 side chains are represented in the set of low-energy conformations of **1** (Figure 1). Further, the measured vicinal coupling constants of the Tyr^1 and Phe^3 side chain protons, H-$C^\alpha C^\beta$-H, are in the range of 6.5−9.0 Hz, consistent with dynamic averaging. In addition to the side chains, the exocyclic peptide group (between the Tyr^1 and D-Cys^2 residues) may also assume different orientations (possible values of the Tyr^1 ψ and D-Cys^2 φ torsion angles are represented in Table 1). This leads to a variety of orientations of the entire Tyr^1 residue relative to the rest of the molecule (Figure 1).

Table 1. Torsion Angles (deg) of 20 Computed Low-Energy Conformations of 1 (Average values ± rms deviations for families A−C)

		structure		
		A	B	C
N^a		13	5	2
$\Delta E_{min}{}^b$		0.1	0.0	1.3
Tyr^1	ψ	153 ± 13	141 ± 8	143 ± 6
		−77 ± 1	−56[c]	
D-Cys^2	φ	157 ± 5	160 ± 5	166 ± 2
		75 ± 5	85 ± 9	
	ψ	36 ± 3	48 ± 2	46 ± 1
	χ^1	−57 ± 2	178 ± 2	178 ± 2
	χ^2	−148 ± 1	150 ± 4	71 ± 1
	χ^3(S−S)	93 ± 1	−103 ± 1	87 ± 1
Phe^3	φ	−83 ± 3	−83 ± 4	−79 ± 5
	ψ	−38 ± 4	−24 ± 5	−49 ± 5
D-Pen^4	φ	138 ± 2	138 ± 1	131 ± 1
	χ^1	−71 ± 1	−70 ± 1	48 ± 2
	χ^2	52 ± 1	91 ± 5	−143 ± 1

[a] N is the number of conformations, in each family, with relative energy ΔE < 3 kcal/mol. [b] ΔE_{min} is the relative energy (kcal/mol) of the lowest energy conformer in the given family. [c] This angle was represented by a single conformation of 1 within the energy interval 0−3.0 kcal/mol.

One approach to identify the features of the bioactive conformation from among this multitude of possibilities is by the incorporation of a series of conformationally constrained analogues of Tyr and Phe in which different regions of conformational space are allowed for the pharmacophoric elements. Given at least some examples of sufficiently active analogues with such replacements, correlation of biological activity with accessible conformations allows features of the bioactive conformation to be deduced. Several conformationally restricted replacements for Tyr and Phe have seen increasing use in such applications. Among these are tetrahydroisoquinoline-3-carboxylic acid (Tic),[8] 2-aminotetralin-2-carboxylic acid (Atc),[9] and 2-aminoindan-2-carboxylic acid (Aic),[9] as phenylalanine replacements,

Table 2. Opioid Binding Affinities of Residue 1 Analogues of JOM-13 (1)[a]

no.	structure	K_i (nM) [^{3}H]DAMGO	K_i (nM) [^{3}H]DPDPE	$K_i(\mu)/K_i(\delta)$
1	Tyr-c[D-Cys-Phe-D-Pen]OH (JOM-13)	52 ± 4.4	0.74 ± 0.08	70
2	Hat-c[D-Cys-Phe-D-Pen]OH	230 ± 17	20 ± 4.4	12
3	D-Hat-c[D-Cys-Phe-D-Pen]OH	310 ± 22	24 ± 5.1	13
4	Hai*-c[D-Cys-Phe-D-Pen]OH	840 ± 40	13 ± 1.2	65
5	D-Hai*-c[D-Cys-Phe-D-Pen]OH	>10000	1700 ± 120	>6.0
6	HO-Tic-c[D-Cys-Phe-D-Pen]OH	>10000	2400 ± 440	>4.2
7	*t*-Hpp*-c[D-Cys-Phe-D-Pen]OH	110 ± 19	0.66 ± 0.06	170
8	D-*t*-Hpp*-c[D-Cys-Phe-D-Pen]OH	~10000	84 ± 6.2	~120
9	*c*-Hpp*-c[D-Cys-Phe-D-Pen]OH	720 ± 57	2.4 ± 0.18	300
10	D-*c*-Hpp*-c[D-Cys-Phe-D-Pen]OH	4440 ± 1660	340 ± 65	13
11	D-Tyr-c[D-Cys-Phe-D-Pen]OH	>10000	1200 ± 140	>8.3
12	α-MeTyr-c[D-Cys-Phe-D-Pen]OH	>10000	2100 ± 240	>4.8
13	NMeTyr-c[D-Cys-Phe-D-Pen]OH	180 ± 9.8	2.4 ± 0.24	75

[a] An asterisk denotes the tentative stereochemical assignment of the α center (see text).

and their appropriate aryl ring-hydroxylated counterparts, 1,2,3,4-tetrahydro-7-hydroxyisoquinoline-3-carboxylic acid (HO-Tic),[10] 6-hydroxy-2-aminotetralin-2-carboxylic acid (Hat),[11,12] and 6-hydroxy-2-aminoindan-2-carboxylic acid (Hai),[11] respectively, as tyrosine replacements (Figure 2). All three types of modification are effective in limiting orientational freedom of χ^1, the angle about the $C^\alpha-C^\beta$ bond, due to the inclusion of this bond in a 5- or 6-membered ring. Due to their bicyclic structures, these modifications also greatly limit the allowed values of χ^2, the dihedral angle about $C^\beta-C^\gamma$. We have recently described the synthesis and use of an additional conformationally restricted Tyr analogue based upon proline, *trans*-3-(4′-hydroxyphenyl)proline (*t*-Hpp).[13] Like HO-Tic, Hat, and Hai, *t*-Hpp limits orientational freedom about χ^1, but unlike these bicyclic tyrosine analogues, rotation about χ^2 is allowed. Substitution of Tyr^1 in **1** by *t*-Hpp does not impede δ receptor binding affinity,[13] indicating that the more limited conformational space available to this residue compared with Tyr includes the orientation required for δ receptor recognition. In the present report we compare the results obtained with *t*-Hpp^1 substitution in **1** with those observed with other conformationally constrained residue 1 substitutions. Included among these is *cis*-3-(4′-hydroxyphenyl)proline (*c*-Hpp), the synthesis of which we report below. The results reveal that while substitution of Tyr^1 by some conformationally constrained analogues does not result in deleterious effects on δ receptor binding, other substitutions lead to moderate or pronounced reductions in affinity. Detailed conformational search/molecular mechanics studies on these analogues are also described, from which the features of the bioactive conformation of residue 1 in **1** and its analogues can be proposed.

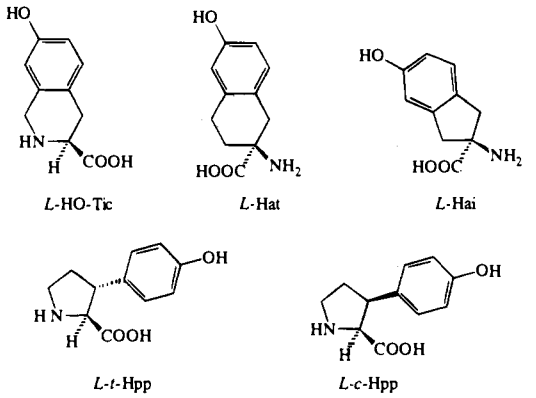

Figure 2. Structures of conformationally restricted tyrosine analogues.

Results and Discussion

Receptor Binding and Bioassay Results. Binding affinities of the residue 1-modified opioid tetrapeptides in competition with radiolabeled ligands selective for the δ ([^{3}H]DPDPE) or μ ([^{3}H]DAMGO) opioid receptor are summarized in Table 2. Peptide affinities for the κ opioid receptor also were assessed in competition binding experiments employing the κ receptor selective ligand [^{3}H]U69,593; however none of the peptides tested showed significant affinity for this receptor (K_i > 10 μM in all cases). The effect on binding affinity of several conformationally restricted Tyr analogues, whose structures are depicted in Figure 2, was examined. Tyr analogues included examples in which bicyclic structures were formed *via* cyclization of the phenolic aromatic to the α carbon (Hat and Hai) or the amine nitrogen (HO-Tic) as well as examples of phenol-substituted prolines (*t*-Hpp and *c*-Hpp). As suggested in Table 2, several of the peptides were prepared using a racemic mixture of the conformationally restricted Tyr analogue which leads to ambiguity in the stereochemical assignment of this residue in each member of the resulting diasteromeric pair of peptides. In each of these pairs, the Hai^1 analogues (**4** and **5**), the *t*-Hpp^1 analogues (**7** and **8**), and the *c*-Hpp^1 analogues (**9** and **10**), one member displays approximately 100-fold higher δ binding affinity than does the other. Since, as for most opioid peptides, the L-Tyr^1 parent peptide, **1**, exhibits much higher δ binding affinity than does the corresponding D-Tyr^1 diastereomer, **11**, we tentatively conclude that the higher affinity analogue (**4**, **7**, and **9**) in each of these three pairs of residue 1-modified diastereomers is that with L-stereochemistry for this residue. The computational results, described below, are consistent with these assignments.

Analogues **2**–**5** are examples in which conformational restriction of the side chain is effected through formation of a bicyclic structure *via* cyclization to the α carbon (Figure 2). In each case, orientational freedom of χ^1, the angle about the $C^\alpha-C^\beta$ bond, as well as orientational freedom of χ^2, the angle about the $C^\beta-C^\gamma$ bond, is greatly reduced. As shown in Table 2, analogues **2**–**4** all display moderate δ binding affinities which are approximately 15–30-fold lower than that observed for the parent peptide, **1**. Analogue **5**, on the other hand, shows considerably lower affinity for the δ receptor and

Table 3. Bioassay Data for Residue 1 Analogues of JOM-13 (1)

no.	structure	IC_{50} (nM) GPI	IC_{50} (nM) MVD	IC_{50}(GPI)/IC_{50}(MVD)
1	Tyr-c[D-Cys-Phe-D-Pen]OH (JOM-13)	460 ± 190	4.2 ± 1.0	110
2	Hat-c[D-Cys-Phe-D-Pen]OH	1800 ± 380	110 ± 45	16
3	D-Hat-c[D-Cys-Phe-D-Pen]OH	4300 ± 1400	340 ± 76	13
4	Hai-c[D-Cys-Phe-D-Pen]OH	>10000	340 ± 160	>29
7	*t*-Hpp-c[D-Cys-Phe-D-Pen]OH	770 ± 26	1.6 ± 0.26	480
9	*c*-Hpp-c[D-Cys-Phe-D-Pen]OH	12000 ± 1400	75 ± 14	160
13	NMeTyr-c[D-Cys-Phe-D-Pen]OH	480 ± 250	5.7 ± 2.0	84

accordingly is tentatively assigned as the D-Hai[1] analogue as discussed above. Unlike the Hai[1] analogues, the Hat[1] analogues **2** and **3** both display similar, moderate binding affinities. This finding indicates that for this conformationally restricted Tyr analogue, both D- and L-stereochemistries allow reasonable superimposition of the key elements of the δ pharmacophore contained within the Tyr residue, namely the α-amino group and the phenolic aromatic and hydroxyl elements.

The reduced δ receptor binding affinities displayed by **2**–**4** suggest that the ideal bioactive conformation is relatively unfavored in these analogues and/or that the additional structural features of the bicyclic system lead to unfavorable (presumably steric) interactions with the receptor. The poor δ binding affinity for the α-MeTyr[1] analogue, **12**, which retains the conformational perturbation of α,α-disubstitution present in **2**–**4** without otherwise constraining the phenolic side chain, is indicative of an adverse interaction between the α-methyl and the receptor. (Computational studies, described below, do not indicate altered conformational preferences for residue 1 in the α-MeTyr[1] analogue.) In view of this observation, it can be proposed that the improved δ affinity displayed by **2**–**4** is indicative of energetically favored bioactive conformations relative to the less constrained analogue **12**. Alternatively or additionally, the presence of the second α-substituent within a ring system in **2**–**4** may alter the geometry of this substituent in such a way as to mitigate the adverse steric effect observed in **12**. These possibilities are discussed further below.

The residue 1 substitution for analogue **6** is an example of a different type of bicyclic structure, one in which cyclization is effected through the α-amino group of the amino acid. In contrast to the moderate δ affinity observed for **2**–**4**, analogue **6** binds poorly to all opioid receptors. The high δ affinity seen for the NMeTyr[1] analogue, **13**, clearly shows that the poor binding of **6** does not result from the replacement of the primary amine of Tyr with a secondary amine. The most likely explanation for the low affinity of **6** is that the conformational constraint imposed by the tetrahydroisoquinoline structure, which confines orientations of the side chain to regions of space different from those permitted in residue 1 of analogues **2**–**4**, precludes low-energy access to the binding conformation for this residue.

As we have discussed previously,[13] the Tyr replacements incorporated into analogues **2**–**6** not only restrict orientation about χ^1 but also, because of their bicyclic structures, greatly limit conformational possibilities for χ^2. This simultaneous restraint of χ^1 and χ^2 not only hinders the straightforward interpretation of reduced affinity but also increases the likelihood of observing reduced affinity since the limited variability of both side chain angles must comply with the binding requirements. The Tyr replacements incorporated into analogues **7**–**10** represent an alternative approach toward side chain restriction. In these analogues, a *p*-hydroxyphenyl-substituted proline (Figure 2) replaces the Tyr[1] residue; consequently, orientational freedom about χ^1 is reduced while rotational freedom about χ^2 is maintained. As we have previously reported,[13] the conformational constraints imposed by replacing Tyr[1] with *t*-Hpp[1] are consistent with the conformational requirements for δ receptor binding since the affinity observed for the *t*-Hpp[1] analogue, **7**, is indistinguishable from that of the parent peptide, **1**. In analogue **9** (which, like **7**, is tentatively assigned to have L-stereochemistry for residue 1 on the basis of affinity comparisons with **10** and **8**, respectively), the Tyr[1] residue is replaced with *c*-Hpp[1] in which the orientation of the phenolic ring relative to the amine nitrogen now differs from that in the *t*-Hpp[1] analogue, **7**. Nonetheless, **9** also displays high δ receptor binding affinity similar to the parent peptide, **1**. As discussed below, this result has important implications for the development of a δ receptor binding model since it requires that the limited and different conformational space available to the *c*-Hpp[1] and *t*-Hpp[1] residues must in both cases include the conformational features required for δ receptor binding.

Analogues **1**–**4**, **7**, **9**, and **13**, all of which display moderate to high binding affinity to the δ opioid receptor, were further examined in bioassays to assess their pharmacological selectivities and determine whether these analogues functioned as agonists or antagonists. The standard μ receptor sensitive guinea pig ileum (GPI)[14] and δ sensitive mouse vas deferens (MVD)[15] assays were employed, and the observed results are summarized in Table 3. All analogues tested were full agonists in both assays (with the possible exception of **4** for which a full dose–response profile was not attained in the GPI) and, as expected from the binding results, were more potent in the MVD than in the GPI assay. While bioassay selectivities (Table 3) were in good agreement with binding selectivities (Table 2), some interesting differences were observed in comparisons of bioactivity potency with binding affinity. For analogues **1**, **2**, **7**, and **13**, MVD potencies correlated well with δ binding affinity, exhibiting ratios of IC_{50}(MVD)/K_i(δ) in the range of 2.5–5.5. By contrast, MVD potencies for **3**, **4**, and **9** were comparatively lower with ratios of IC_{50}(MVD)/K_i(δ) in the range of 14–30. Of particular interest is the comparison of results observed for **7** and **9**, the [*t*-Hpp[1]]-and [*c*-Hpp[1]]JOM-13 analogues, respectively. As indicated in Table 2, both analogues bind avidly to the δ opioid receptor; however, as seen from Table 3, **7** displays almost 50-fold higher MVD potency than **9**. One possible explanation for this discrepancy is that **9** (as well as **3** and **4**) possesses lower efficacy than does **7** (as well as **1**, **2**, and **13**) and must occupy a

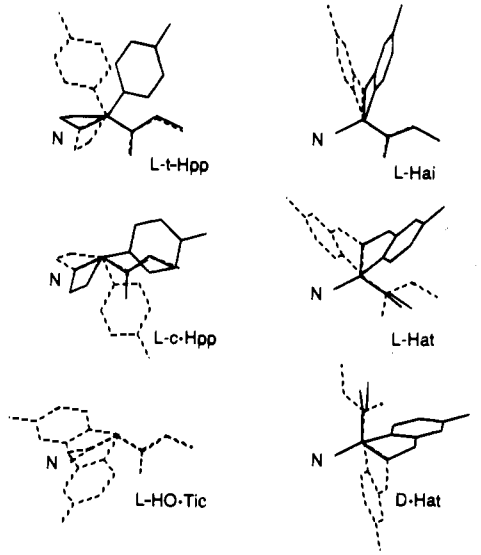

Figure 3. Superposition of possible *trans* (solid line) and *gauche* (dashed line) side chain rotamers (relative to $C^{\alpha}-C^{\beta}$ bond) of *t*-Hpp, *c*-Hpp, Hai, Hat, and HO-Tic methylamides. N^{α}, C^{α}, and C^{β} atoms were used for superposition.

Table 4. Torsion Angles χ^1 and χ^2 (deg), Relative Energies ΔE (kcal/mol), and Distances d_{N-O} between N^{α} and O^{η} Atoms (Å) for Modified Tyr Methylamides

residue	rotamer	χ^1	χ^2	ΔE	d_{N-O}
t-Hpp	*trans*	−151	64	0.0	7.7
	gauche$^+$	−91	68	2.0	6.8
c-Hpp	*trans*	165	99	1.8	7.8
	gauche$^-$	88	−66	0.0	6.8
Hai	*trans*	−134	9	0.0	7.2
	gauche$^+$	−97	−13	0.2	6.5
Hat	*trans*	−168	20	0.3	7.9
	gauche$^+$	−71	−20	0.0	6.6
D-Hat	*trans*	168	−20	0.1	7.9
	gauche$^-$	71	20	0.0	6.6
HO-Tic	*gauche*$^+$	−36	41	0.0	5.9
	gauche$^-$	30	−39	0.3	6.0

greater proportion of δ receptors in the MVD to elicit a comparable response. For analogues with varying conformational constraints, such differences in efficacy are not unexpected since the effects of the differing constraints on binding and transduction may diverge. Thus, two differing conformational constraints both may be consistent with high-affinity binding but not with optimal efficacy. Indeed, similar discrepancies between binding and bioassay results have been reported for other conformationally restricted opioid peptides.[16,17] An alternate explanation for the bioassay discrepancies observed can be proposed on the basis of δ opioid receptor subtypes. Considerable evidence for such δ subtypes has accrued recently from *in vivo* studies which have pointed to the existence of two δ subtypes, δ_1 and δ_2, in the central nervous system.[18-22] Recently, it has been shown that the functional receptor in the MVD bioassay is the δ_2 subtype;[23] hence the potency differences observed for analogues **3**, **4**, and **9** compared with analogues **1**, **2**, **7**, and **13** may reflect differing δ subtype selectivities which are not readily observable in the binding assays employing brain tissue. Further investigations will probe these possible explanations.

Theoretical Conformational Analysis of Tetrapeptides. Figure 3 and Table 4 show the low-energy side chain conformations of the conformationally constrained tyrosine analogue amino acid methylamides. Compared with tyrosine, incorporation of additional ring structures into the first residue strongly constrains the flexibility of its side chain. Each Tyr^1 analogue has only two low-energy side chain orientations about the $C^{\alpha}-C^{\beta}$ bond which differ among the set of conformationally restricted amino acids. For each of the constrained Tyr^1 replacements except HO-Tic, one side chain conformer is *gauche* and the other *trans* about the $C^{\alpha}-C^{\beta}$ bond. In the case of HO-Tic, both conformers are *gauche*. By contrast, for α-MeTyr, in which the side chain has no second tether to the backbone, all three standard conformers ($\chi^1 = \pm 60°$ and 180°) are accessible.

All the side chain conformers of the isolated amino acid shown in Figure 3 and Table 4 are also accessible when these amino acids are incorporated into tetrapeptide analogues of **1**. Similar to the parent peptide, conformations of these analogues may be described simply as all possible combinations of the A, B, and C tripeptide cycle structures mentioned above, side chain conformers of the modified first residue and Phe^3 residue, and conformers of the first peptide group (i.e., torsion angles ψ of Tyr^1 and φ of D-Cys^2) which define the orientation of the first residue relative to the cycle. As examples, the low-energy conformers of the *t*-Hpp^1 and Hai^1 analogues of **1** are shown in Figures 4 and 5. The phenolic ring in the *t*-Hpp^1 analogue, **7**, occupies a limited "fan-shaped" sector of space (Figure 4) that is smaller than observed for **1** (Figure 1), but this conformationally accessible sector is still sizable due to flexibility of the exocyclic peptide group between the *t*-Hpp^1 and D-Cys^2 residues and the existence of two distinct side chain conformers of the *t*-Hpp^1 residue. Similar observations hold for the *c*-Hpp^1 analogue, **9** (not shown). For the *t*-Hpp^1 and *c*-Hpp^1 residues, the χ^1 and χ^2 torsion angles (Table 4) are close to standard values for rotamers of the Tyr side chain (±60° and 180° for χ^1 and ±90° for χ^2). Consequently, all conformers of the *c*-Hpp^1 and *t*-Hpp^1 analogues are almost identical geometrically to corresponding conformers of the parent peptide, **1**. For these residues, the incorporation of the additional cycle, however, eliminates the *gauche*$^+$ (for *c*-Hpp^1) or *gauche*$^-$ (for *t*-Hpp^1) side chain conformers and changes the relative energies of the remaining *gauche* and *trans* side chain rotamers: the *trans* rotamer is energetically preferred for *t*-Hpp^1 (by 2 kcal/mol, Table 4) and has greater representation in the set of low-energy conformations of the corresponding peptide (Figure 4), while the *gauche* rotamer is preferred for the *c*-Hpp^1 analogue (by 1.8 kcal/mol, Table 4). It should be noted that low-energy conformations with a *trans* orientation of the residue 1 side chain are found for the parent peptide and both its high affinity Hpp^1 analogues.

Similar to the Hpp^1 analogue, each of the HO-Tic^1, Hai^1, and Hat^1 analogues of **1** has two different side chain conformers of residue 1 with χ^1 close to ±60° or 180°; the maximum deviation (~46°) of χ^1 from the standard values was observed for the *trans* conformer of the Hai^1 analogue (Table 4). However, the χ^2 angle of residue 1 in the HO-Tic^1, Hai^1, and Hat^1 analogues is fixed near ±20° (Table 4, Figure 3) because of the participation of the aromatic rings in bicyclic structures. The residue 1 aromatic rings in these analogues can be described as occupying "funnel-like" regions of space (Figure 5), in which the tilt of the "funnel" relative to

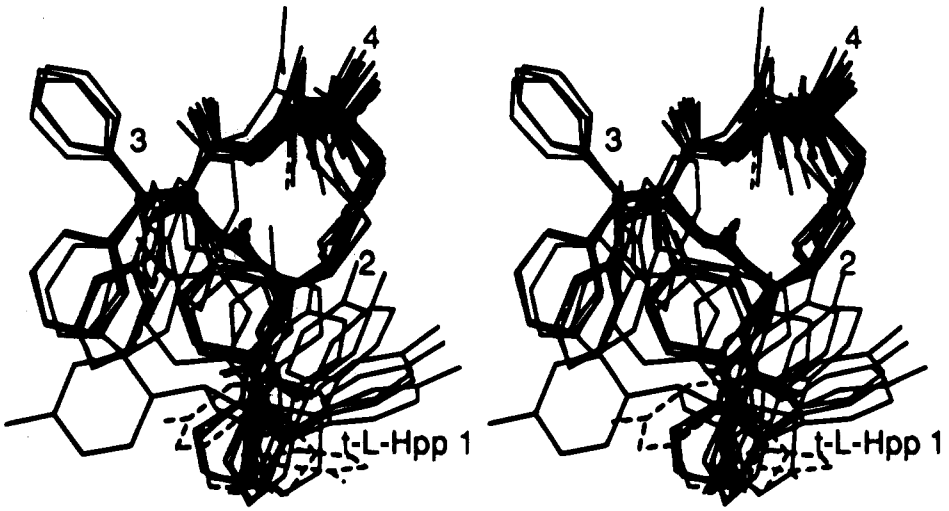

Figure 4. Superposition (stereoview) of 15 [*t*-Hpp^1]JOM-13 conformers with relative energies ΔE < 4 kcal/mol. The conformers with χ^1 of *t*-Hpp^1 ~ −90° (*gauche*$^+$) are indicated by dashed lines.

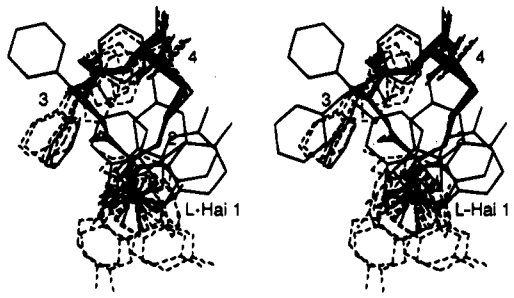

Figure 5. Low-energy (ΔE < 3 kcal/mol) conformers of [Hai^1]-JOM-13 which correspond to the lowest energy configuration of the disulfide bridge. Conformers with χ^1 of Hai^1 ~ −90° (*gauche*$^+$) are indicated by dashed lines.

the rest of molecule depends on the particular modification (HO-Tic^1, Hai^1, and Hat^1 or D-Hat^1) of the side chain and on its (*gauche* or *trans*) conformer.

The α-MeTyr^1 analogue of **1** has almost the same set of low-energy conformations as the parent peptide since the additional α-methyl group does not constrain the flexibility of either the side chain of residue 1 or the peptide group between residue 1 and the rigid tripeptide cycle. The addition of the α-methyl group in the α-MeTyr^1 analogue (as well as the similar α-methylene group in the Hai^1 and Hat^1 analogues) has little influence on the conformation of the first peptide group because the energetically preferred values of the ψ backbone torsion angle for Tyr^1 in the parent peptide, **1** (~ −60° and 160°, see Table 1), are close to those in α-methylated residues (±60° and 180°).[24]

The general conformational features of the residue 1-modified analogues of **1** can be described as follows. 1. The nature of the Tyr^1 modification has little influence on backbone and disulfide bridge conformers within the rigid cycle D-Cys-Phe-D-Pen. The changes in relative energies of the A and B conformers due to the residue 1 substitutions are less than 0.5 kcal/mol. This is in agreement with the fact that relative occupancies and chemical shifts of the two slowly exchangeable conformers, A and B, observed for **1** and its analogues in solution do not change significantly throughout a series encompassing numerous chemical modifications to the side chains of the first residue of JOM-13 (K. Sobczyk-Kojiro and H. I. Mosberg, unpublished observations). 2. Low-energy conformations of the first exocyclic peptide group (i.e., the energetically preferable torsion angles ψ of Tyr^1 and φ of D-Cys^2) are very similar in all the residue 1-substituted analogues of **1** (the differences in these torsion angles are <30°). They are not substantially altered either by methylation of the Tyr C$^\alpha$ atom or by inclusion of additional 5- and 6-membered rings *via* the C$^\alpha$ or N$^\alpha$ atoms of Tyr^1. 3. For the residue 1 replacements incorporating additional ring structures (*c*-Hpp, *t*-Hpp, Hat, D-Hat, Hai, and HO-Tic), only two side chain conformers, which depend on the nature of the additional ring, are possible. As a result, the Tyr^1 aromatic ring occupies different areas of space which are more limited than in the parent peptide.

Conformational Requirements for δ Binding. All the peptides with a modified first residue can be classified into three groups according to their binding affinities for the δ opioid receptor (Table 2): high-affinity analogues (residue 1 = Tyr, *c*-Hpp, and *t*-Hpp; K_i ~ 0.74, 2.4, and 0.66 nM, respectively), moderate affinity analogues (Hai, Hat, and D-Hat; K_i ~ 13, 20, and 24 nM, respectively), and inactive analogues (α-MeTyr and HO-Tic; both with K_i ~ 2000 nM). The search for the δ receptor-bound conformation of **1** was based on the assumption that all high- and moderate affinity analogues have similar arrangements of functionally important groups, the most important of which are the positively charged N$^\alpha$ nitrogen of Tyr^1 (or replacement) and the side chains of the Tyr^1 (or replacement) and Phe^3 residues. Within the first residue side chain, both aromaticity and the *para* phenolic functions are required for high binding affinity.[25] The relative arrangement of the two functionally important groups (N$^\alpha$ nitrogen and phenolic ring) of this residue depends only on the χ^1 and χ^2 torsion angles. Therefore, the initial search for a common δ receptor-bound conformation was performed for the first residue alone, independent of the rest of the molecule, to identify the χ^1 and χ^2 torsion angles which provide superposition of the N$^\alpha$ nitrogen and the phenolic ring in the high- and moderate affinity analogues. In the next stage, superposition of the entire peptide molecules was done to provide additional overlap of the Phe^3 aromatic rings.

For the high-affinity peptides, the required common conformation of the first residue may be easily derived

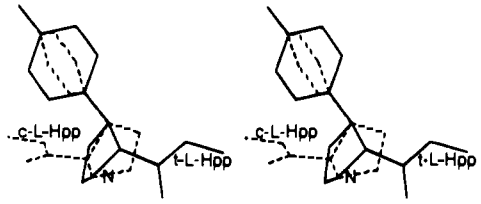

Figure 6. Superposition of *gauche* conformers of *t*-Hpp methylamide (solid line, $\chi^1 = -91°$) and *c*-Hpp methylamide (dashed line, $\chi^1 = +88°$).

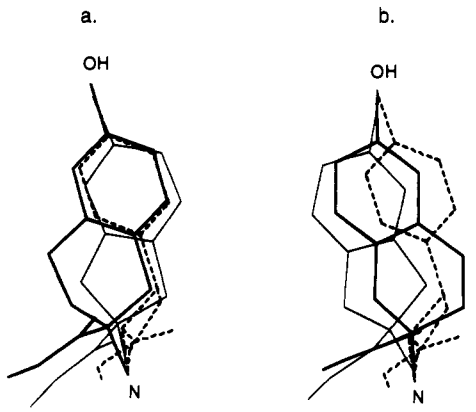

Figure 7. Superposition of *trans* conformers of (a) *t*-Hpp methylamide (dashed line), Hat methylamide (bold solid line), and Hai methylamide (solid line) and (b) *t*-Hpp methylamide (dashed line), D-Hat methylamide (bold solid line), and D-Hai methylamide (solid line).

from comparison of *c*-Hpp and *t*-Hpp methylamides. The N^{α} group and the aromatic ring of these residues may be in *gauche* or *trans* orientations around the $C^{\alpha}-C^{\beta}$ bond (Figure 3, Table 4). These two different conformers cannot be well superimposed because the distances between the functionally important N^{α} and O^{η} atoms differ by ~1 Å (Table 4). *Gauche* rotamers of *c*-Hpp and *t*-Hpp differ in the sign of the χ^1 angle (~ +90 and −90°, respectively). Therefore their superposition (Figure 6) leads to different orientations of the Tyr[1] aromatic rings, different directions of the peptide group between Tyr[1] and D-Cys[2] residues, and, as a result, different arrangements of the first residue relative to the rest of the molecule. On the other hand, *trans* conformers of the first residue ($\chi^1 = 167°$ in *c*-Hpp and −145° in *t*-Hpp) provide complete superposition of N^{α} atoms, aromatic ring, and peptide groups in these high-affinity analogues with individual deviations of all functionally important atoms in the tyramine part of the residue (N^{α}, O^{η}, $C^{\epsilon 1}$, $C^{\epsilon 2}$, and C^{η}) <0.3 Å. The *trans* orientation is the energetically preferable one for the *t*-Hpp[1] analogue, **7**, but is of higher energy (compared to the *gauche*$^-$ conformer) for the *c*-Hpp[1] analogue, **9** (Table 4). This may explain the slightly lower affinity of the latter analogue in comparison with the former (2.4 vs 0.66 nM, Table 2). Thus, the *trans* conformer of the Tyr[1] analogue side chain with $\chi^1 \sim 180°$ and $\chi^2 \sim 90°$ may be deduced to be that existing in the δ receptor-bound conformation for the high-affinity peptides.

For moderate affinity peptides, the δ receptor-bound conformation of the tyramine fragment is also most probably *trans* since this provides a similar distance between the functionally important NH_3^+ and $O^{\eta}H$ groups (7.2−7.9 Å) as is observed in the high-affinity peptides (Table 4). With this side chain arrangement, the tyramine portions of the Hat[1] and Hai[1] analogues

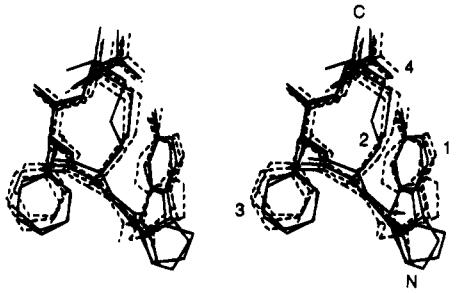

Figure 8. Superposition of candidate δ receptor-bound conformations for high-affinity (*t*-Hpp[1] and *c*-Hpp[1]; solid line) and moderate affinity (Hai[1], Hat[1], and D-Hat[1]; dashed line) analogues of **1**. All conformations represented (from Table 3) have torsion angles φ of D-Cys[2] ~ 160° and χ^1 of Phe[3] ~ −60°. The functionally important atoms N^{α}, O^{η}, $C^{\epsilon 1}$, $C^{\epsilon 2}$, and C^{η} of residue 1 and the C^{γ} atom of Phe[3] were used for the superposition.

can be very well superimposed with those of the high-affinity peptides (Figure 7a). The inactivity of the HO-Tic[1] analogue can be explained by the different structure observed for its tyramine component in which only *gauche* rotamers are possible (Figure 3) which causes the N^{α} and O^{η} atoms to be located too close together (≤6 Å, Table 4). The tyramine N^{α} and O^{η} atoms of the D-Hat[1] and D-Hai[1] analogues of **1** can also be superimposed with the corresponding atoms of the high-affinity peptides (Figure 7b). However, in this case, the aromatic rings of the D-Hat[1] and D-Hai[1] residues are shifted relative to the ring of *t*-Hpp[1] by ~0.8 and 1.0 Å, respectively (Figure 7b). Consequently, reduced δ binding affinity might be expected for both the D-Hat[1] analogue, **3**, and, especially, the D-Hai[1] analogue, **5**, in which the tyramine ring shift is more pronounced. Indeed, the δ receptor binding affinity of **5** is greatly reduced ($K_i \sim 1600$ nM). Interestingly, however, **3** displays moderate binding affinity (24 nM) which is comparable to that of the L-Hat[1] analogue, **2**. This moderate affinity is likely due to the better superposition of the tyrmaine portion of the D-Hat[1] analogue (compared to the D-Hai[1] analogue) with the corresponding region of the high-affinity analogues (Figure 7b). Similar observations of inferior superpositioning of analogues with D-amino acids in residue 1 (results not shown) support the tentative stereochemical assignments in Tables 2 and 3.

The results above define the δ receptor-bound conformations of the tyramine fragments (χ^1 and χ^2 torsion angles) for **1** and its high- and medium affinity analogues. The χ^1 torsion angle of Tyr[1] (or Tyr[1] replacement) is ~180° ± 30° for all the peptides (−134° for Hai[1] in **4**, Table 4), while the χ^2 torsion angles depend on the type of additional cycle incorporated into the first residue (Table 4). In the next stage of computations, possible δ receptor-bound conformations of the whole peptide molecule (i.e., the Tyr[1] ψ, D-Cys[2] φ, and Phe[3] χ^1 torsion angles) were identified. To do this, all the previously obtained low-energy conformers of the different peptides (Figures 4 and 5) with the χ^1 angle of the first residue ~180° were compared by superimposing their tyramine functions to define which conformers also provide overlap of the Phe[3] aromatic rings. The resulting low-energy conformers of the peptides which provide the best superposition of all phamacophoric elements are represented in Figure 8 and Table 5. The superposition depicted (Figure 8) provides coordinate root mean square deviations of functionally important groups

Table 5. Relative Energies ΔE (kcal/mol) and Torsion Angles (deg) of Possible δ Receptor-Bound Conformations of 1 and Its Analogues with Constrained First Residue

residue 1		Tyr^1	*t*-Hpp^1	*c*-Hpp^1	L-Hai^1	L-Hat^1	D-Hat^1
ΔE^a		0.1	0.0	0.6	1.2	2.6	0.4
X^1	ψ	138	155	152	162	163	135
	χ^1	−167	−158	167	−142	−168	162
	χ^2	80	61	99	14	45	−14
D-Cys^2	φ	165	158	164	147	156	164
	ψ	41	39	50	30	39	38
	χ^1	−58	−57	177	−51	−58	−53
	χ^2	−148	−148	149	−150	−149	−151
	χ^3	94	94	−102	93	93	95
Phe^3	φ	−85	−85	−86	−84	−85	−91
	ψ	−40	−40	−23	−35	−40	−36
	χ^1	−59	−65	−56	−70	−75	−75
	χ^2	93	88	99	93	79	76
D-Pen^4	φ	141	140	138	141	140	139
	χ^1	−71	−70	−71	−72	−70	−72
	χ^2	52	53	93	50	53	51

[a] ΔE represents the energy difference between represented conformer and lowest energy conformer identified for analogue specified.

in the series of peptides (the set of atoms: N^α, O^η, $C^{\epsilon 1}$, $C^{\epsilon 2}$, and C^η of residue 1 and C^γ of Phe^3) of 0.3−0.4 Å between the high-affinity analogue **7** and the medium affinity analogues and 0.2 Å between **1** and its *t*-Hpp^1 and *c*-Hpp^1 analogues. The Phe^3 aromatic rings of all the peptides are in the same plane, and the deviations of their centers from the reference Phe^3 ring in the *t*-Hpp^1 analogue are <0.4 Å. The cyclic tripeptide fragments of all the peptides are overlapped as well, including the C-terminal COO^- group which is important for δ selectivity.[4,26] In general, the high-affinity analogues can be better superimposed with each other than with the moderate affinity analogues.

The candidate δ receptor-bound conformations represented in Figure 8 and Table 5 share an extended structure of the exocyclic peptide group (both torsion angles ψ of residue 1 and φ of D-Cys^2 are close to 160°) and a Phe^3 side chain rotamer with $\chi^1 \sim -60°$. This orientation of the Phe^3 side chain, however, is for illustrative purposes only. Other values of the Phe^3 χ^1 angle (~+60° or 180°, for example) can provide equally good overlap of the Phe^3 aromatic rings in all peptides considered because the Phe^3 C^α−C^β bonds coincide in the represented superposition (Figure 8). Further, all three conformers of the disulfide bridge (A−C in Table 1) have an identical mutual arrangement of the Tyr and Phe residues. Consequently, the lowest energy conformer of the disulfide bridge for each peptide was chosen simply to represent its probable bound conformation in Table 5. The candidate backbone δ receptor-bound conformation is deduced to have a ψ of residue 1 and a φ of D-Cys^2 ~ 160° since this provides much better superposition of the pharmacophore elements than all other low-energy conformers. As an example, the best superposition of conformations with the alternative low-energy value of the φ angle for D-Cys^2 (~70°) is represented in Figure 9 for the *t*-Hpp^1 and Hai^1 analogues. In this case, the functionally important aromatic rings of the Tyr equivalent residues have different orientations in the high- and moderate affinity compounds shown although distances between them are similar. As a result, the coordinate root mean square deviation of all 14 pharmacophore atoms (carbons of residue 1 and Phe^3 aromatic rings and N^α and O^η atoms of residue 1) between the conformations of the *t*-Hpp^1

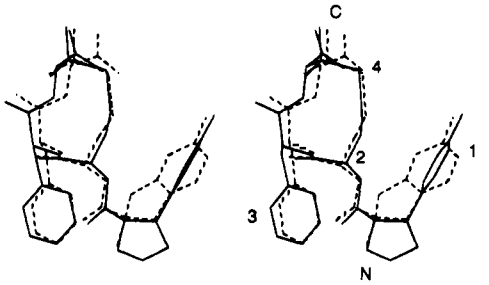

Figure 9. Superposition of alternative conformations with torsion angle φ of D-Cys^2 ~ 70° for [*t*-Hpp^1]JOM-13 (solid line; $\varphi_2 = 75°$, $\Delta E = 1.0$ kcal/mol) and [Hai^1]JOM-13 (dashed line; $\varphi_2 = 66°$, $\Delta E = 0.4$ kcal/mol). The N^α and O^η atoms of residue 1 and the carbons of the residue 1 and Phe^3 aromatic rings were used for the superposition.

and Hai^1 analogues is 0.6 Å in comparison with 0.3 Å for the same atom set in the conformations represented in Table 5 and Figure 8. It should also be noted that, in addition to producing generally poorer superpositions, alternative conformations with the ψ of residue 1 ~−60° have relative energies >3.5 kcal/mol for the high-affinity *c*-Hpp^1 analogue, making such values of ψ unlikely in the δ receptor-bound conformer.

The α-MeTyr^1 analogue displays very poor binding (K_i ~ 2000 nM) despite its conformational identity with the high-affinity parent peptide, **1**. The likely explanation is the existence of some steric hindrance between the additional α-methyl group and the corresponding region of the δ receptor binding site. The Hat^1 and Hai^1 analogues have similar α-CH_2 groups within their aliphatic 6- or 5-membered rings; however these α-CH_2 groups are shifted 0.6 and 1.4 Å, respectively, relative to the position of the α-CH_3 group in [α-MeTyr^1]JOM-13 after superposition of corresponding conformations. This shift of position of the α-substituent may lessen the adverse steric interaction at the δ receptor. Furthermore, the aliphatic rings in Hat and Hai fix the aromatic ring of the first residue in an appropriate binding orientation, providing improved binding due to an entropic contribution. As a result of these effects, the δ binding constants of these bicyclic, α-substituted peptides are improved relative to [α-MeTyr^1]JOM-13.

Although the exact orientation of the Phe^3 aromatic ring in the bound state of the cyclic tetrapeptides considered here still remains undefined, some general features of the δ receptor-bound conformation can be inferred from our results. All three important pharmacophoric elements of **1**, i.e., the Tyr^1 NH_3^+ group and the aromatic rings of the Tyr^1 and Phe^3 residues, are situated on the same side of the molecule (front side in Figure 10) that is presumably embedded into the binding cleft of the δ opioid receptor. These groups form an almost continuous surface if the χ^1 angle of Phe^3 is ~−60° (Figure 9). The opposite surface of the molecule (back side in Figure 9) consists of hydrophilic main chain carbonyl groups which probably point toward the water solution or interact nonspecifically with the wall of the binding cleft. The charged N- and C-terminal NH_3^+ and COO^- groups of JOM-13 and its analogues are oriented in opposite directions (Figure 10). The COO^- group probably points out of the binding cleft into solution, while the NH_3^+ group is buried deep within the binding cleft, most likely interacting with the aspartic acid residue 128 of the third transmembrane α-helix of δ opioid receptors. This aspartic acid is a

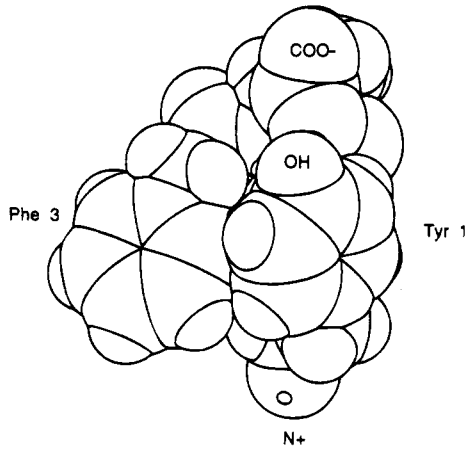

Figure 10. Space-filling model of a candidate δ receptor-bound conformation of JOM-13.

counterion of the positively charged nitrogen in cationic amine receptors[27] and is highly conserved in families of opioid and somatostatin receptors but is usually replaced in other subfamilies of G-protein coupled receptors.

Conclusions

The results presented here represent an example of the use of a series of peptide analogues in which a varying range of conformational constraints within a single residue can be used to elucidate the conformational requirements for bioactivity for that residue. In this example analogues with different conformationally restricted Tyr[1] replacements with differing side chain conformational preferences fall into three categories based on δ opioid receptor binding affinities: high, moderate, and low affinity. Although each analogue still retains many low-energy conformational possibilities, the bioactive conformation must exist in the smaller intersection of possible conformers of all high-affinity analogues. Thus, a reasonable model of the bioactive conformation can be developed more reliably.

The conformational requirements for δ opioid receptor binding in the set of cyclic peptides described here may be summarized as follows. The side chain conformation of residue 1 is *trans*($\chi^1 \sim 180°$) around the $C^\alpha-C^\beta$ bond. The χ^2 angle of this residue is ~90° in Tyr[1], *c*-Hpp[1], and *t*-Hpp[1] analogues and is ~0° in Hat[1] and Hai[1] analogues. The two flexible backbone exocyclic torsion angles (ψ angle of residue 1 and φ angle of D-Cys[2]) are most probably ~160° in the δ receptor-bound conformation. These conclusions can be compared with a recent model[28] of the δ receptor-bound conformation for the parent peptide, **1**, proposed from its superposition with the more flexible cyclic δ selective opioid peptide DPDPE[3] which differs, in part, from **1** by having an additional Gly residue within the disulfide-containing cycle. Our model differs from the previously proposed one by incorporating a definite Tyr[1] side chain conformation (undefined in the previous study), in the conformation of the disulfide bridge, and in the value of the torsion angle φ of the D-Cys[2] residue. While the analysis of residue 1-modified analogues of **1** allows a model for the bioactive conformation of this residue to be proposed, it does not allow the determination of the δ receptor-bound conformation for the side chain of the Phe[3] residue. To remove this remaining uncertainty, further analyses of analogues of **1** with conformationally restricted replacements for the Phe[3] residue are necessary. These analyses are described in the following report.

Experimental Section

General Methods for Peptide Synthesis and Analysis. Protected and unprotected amino acids, except for those the syntheses of which are described below, as well as coupling agents, were purchased from the following commercial sources: Aldrich Chemical Co., Pierce, Bachem Bioscience, Chemical Dynamics Corp., Sigma Chemical Co., Peptides International, Vega Biotechnologies, and Advanced ChemTech. HO-Tic was a generous gift from Prof. Dirk Tourwe. Radioligands were purchased from New England Nuclear or obtained from The National Institute on Drug Abuse Drug Supply Program. Peptides were synthesized by standard solid phase procedures as previously described for the lead tetrapeptide, **1**,[4] using chloromethylated poly(styrene) (Merrifield) resin cross-linked with 1% divinylbenzene. Trifluoroacetic acid (TFA) was employed for deprotection, and dicyclohexylcarbodiimide (DCC) and 1-hydroxybenzotriazole (HOBt) were used as coupling agents. α-Amino functions were protected with the *tert*-butyloxycarbonyl (Boc) group, and *p*-methylbenzyl protection was employed for the labile side chain sulfhydryl groups of Cys and Pen. Deprotection and cleavage from the resin were accomplished by treatment with anhydrous hydrogen fluoride in the presence of 5% cresol and 5% *p*-thiocresol,[29] with stirring for 45 min at 0 °C. HF was subsequently removed by vacuum. Following extraction with 9:1 DMF:80% HOAc and dilution with 0.1% TFA in water, the resulting linear, free sulfhydryl-containing peptides were purified by reverse phase high-performance liquid chromatography (RP-HPLC) on a Vydac 218TP C-18 column (2.5 cm × 22 cm) using the solvent system 0.1% (w/v) TFA in water/0.1% (w/v) TFA in acetonitrile, by a gradient of 10–50% organic component in 40 min. Following lyophilization, treatment of an aqueous solution (pH 8.5) of the linear free sulfhydryl-containing compounds with $K_3Fe(CN)_6$ for ca. 1 h effected cyclization to disulfide analogues. The product cyclic peptides were then purified by RP-HPLC as described above, and pure fractions were pooled and lyophilized. For peptides synthesized using racemic mixtures of conformationally restricted tyrosine analogues, the resulting diasteromeric peptide pairs were separated as the free sulfhydryls since this afforded the maximum resolution. For the Hat[1] and D-Hat[1] peptides, each synthesized from enantiomerically enriched amino acid obtained as described below, separation of the sulfhydryl peptides provided an estimate (based on HPLC peak integration) of the extent of enrichment (enriched D-Hat, 88% D-Hat, 12% L-Hat; enriched L-Hat, 76% L-Hat, 24% D-Hat).

Final peptide purity was determined by analytical RP-HPLC on a Vydac 218TP C-18 column (4.6 mm × 250 mm) by a gradient of 0–70% organic component over 70 min, with a flow rate of 1 mL/min. All analytical RP-HPLC gradients were run using the solvent system 0.1% (w/v) TFA in water/0.1% (w/v) TFA in acetonitrile. Peaks were monitored at 220, 230, 254, and 280 nm and analyzed with Waters Maxima 820 software. Peaks which also appeared in chromatograms in which no peptide was injected were considered to be artifacts and were ignored. Peptide purity was then evaluated by integration of peaks and was found to be >95% for each of the peptides reported here. All newly reported peptides were also subjected to thin layer chromatography (TLC) on precoated silica gel plates in three solvent systems (solvent ratios are v:v): (A) *n*-butanol:acetic acid:water (4:1:5, organic phase only), (B) *n*-butanol:water (containing 3.5% acetic acid and 1.5% pyridine) (1:1, organic phase only), and (C) *n*-amyl alcohol:pyridine:water (7:7:6). In all cases, a single spot was detected using three methods of visualization (ninhydrin, ultraviolet absorption, iodine vapor) for each solvent system.

The absence of free sulfhydryl groups in final product peptides was confirmed by testing with 5,5'-dithiobis(2-nitrobenzoic acid) (Ellman's reagent), which, when combined with free sulfhydryl-containing species, forms an adduct which

Table 6. Physicochemical Data for Cyclized Peptides

peptide analogue	no.	HPLC elution time (min)[a]	TLC R_f[b] A	TLC R_f[b] B	TLC R_f[b] C	FAB-MS MW
Hat-D-Cys-Phe-D-PenOH	**2**	30	0.76	0.73	0.76	586
D-Hat-D-Cys-Phe-D-PenOH	**3**	30	0.74	0.69	0.78	586
Hai-D-Cys-Phe-D-PenOH	**4**	30	0.55	0.51	0.59	572
D-Hai-D-Cys-Phe-D-PenOH	**5**	30	0.54	0.47	0.60	572
HO-Tic-D-Cys-Phe-D-PenOH	**6**	31	0.83	0.69	0.80	572
t-Hpp-D-Cys-Phe-D-PenOH	**7**	30	0.66	0.49	0.76	586
D-*t*-Hpp-D-Cys-Phe-D-PenOH	**8**	30	0.59	0.38	0.69	586
c-Hpp-D-Cys-Phe-D-PenOH	**9**	29	0.59	0.41	0.69	586
D-*c*-Hpp-D-Cys-Phe-D-PenOH	**10**	29	0.55	0.39	0.67	586
D-Tyr-D-Cys-Phe-D-PenOH	**11**	30	0.55	0.54	0.67	560
α-MeTyr-D-Cys-Phe-D-PenOH	**12**	30	0.56	0.52	0.63	574
NMeTyr-D-Cys-Phe-D-PenOH	**13**	31	0.47	0.39	0.63	574

[a] HPLC elution time using a linear gradient of 0–70% organic component in 70 min at a flow rate of 1 mL/min. Solvent system was 0.1% (w/v) TFA in water/0.1% (w/v) TFA in acetonitrile. The solvent front eluted at 3.0 min. [b] R_f values for thin layer chromatograms in solvent systems: (A) *n*-butanol:acetic acid:water (4:1:5, organic component only), (B) *n*-butanol:water (containing 3.5% acetic acid and 1.5% pyridine) (1:1, organic component only), and (C) *n*-amyl alcohol:pyridine:water (7:7:6).

Scheme 1. Syntheses of Boc-*t*-Hpp, **23**, and Boc-*c*-Hpp, **24**

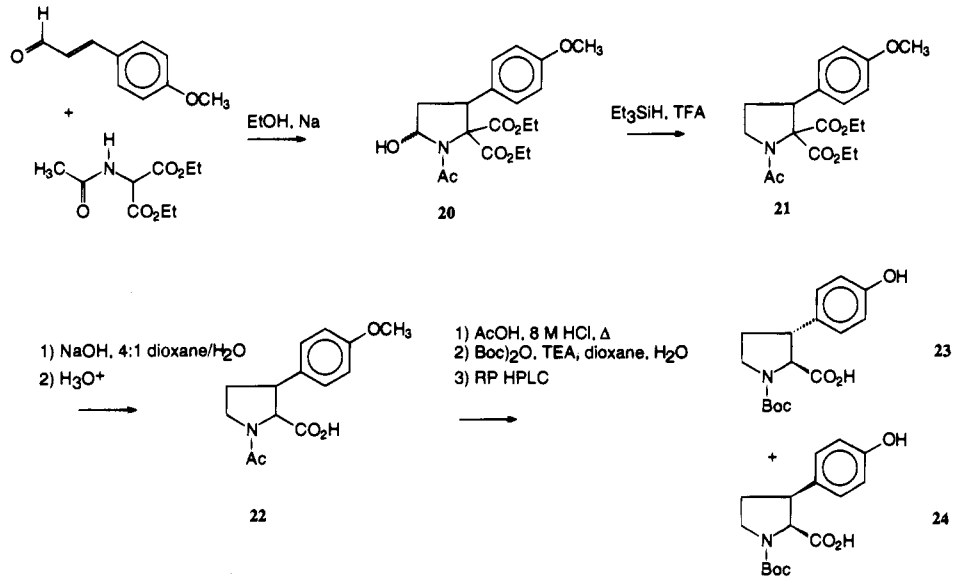

gives a characteristic yellow color and absorbance at 412 nm.[30] In all cases, absorbances of the final peptides at this wavelength were indistinguishable from sulfhydryl-free controls, confirming the absence of free sulfhydryl groups.

^{1}H NMR spectra were registered on General Electric GN-500 and IBM WP 270 SY spectrometers, operating at 500 and 270 MHz, respectively. Samples contained 1–2 mg of the compound in D_2O, acidified (CD_3COOD) D_2O, or DMSO, with 2,2,3,3-tetradeuterio-3-(trimethylsilyl)propionic acid sodium salt (TSP-d_4) added as the internal chemical shift standard. Diagnostic resonances originating from the methyl groups and the α proton of penicillamine and the aromatic resonances of tyrosine (or replacement) and phenylalanine confirmed the presence of these residues. All peptides also displayed NH–αCH–βCH_2 connectivities consistent with the presence of cysteine. No resonances were observed that could not be accounted for, and all resonances pertaining to specifically modified residue 1 amino acids were present. Some analogues were subjected to 2D COSY analysis to establish intraresidue connectivities and/or to 2D NOESY experiments to obtain primary sequences from intraresidue NOE interactions. In each case, the anticipated sequence was confirmed.

Final product confirmation was obtained by fast atom bombardment mass spectrometry (FAB-MS). In all cases, the anticipated molecular weights were confirmed by FAB-MS. The molecular weights determined from FAB-MS along with retention times from HPLC and R_f values from TLC analyses are summarized in Table 6.

Amino Acid Syntheses. Syntheses of 2-amino-5-hydroxyindan-2-carboxylic acid, 2-amino-6-hydroxytetralin-2-carboxylic acid, and their N^{α}-Boc derivatives followed literature procedures.[31,32] The syntheses of N^{α}-Boc-*trans*-3-(4′-hydroxyphenyl)proline and N^{α}-Boc-*cis*-3-(4′-hydroxyphenyl)proline, which are outlined in Scheme 1, were modeled after published syntheses of the corresponding 3-phenylprolines.[33,34]

2-Amino-5-hydroxyindan-2-carboxylic Acid (Hai, 14)[31] and 2-[(*tert*-Butyloxycarbonyl)amino)]-5-hydroxyindan-2-carboxylic Acid (Boc-Hai, 15). 5-Hydroxy-2-spiro[hydantoinindan] (0.2 g, 0.92 mmol), prepared from 2-indanone following the procedure of Pinder et al.,[31] was dissolved in 2 mL of concentrated HCl and heated in a sealed tube at 120 °C for 4 h followed by further heating at 160 °C for 2 h. The solution was then decolorized with activated charcoal, filtered, and rotary evaporated to an off-white solid which was recrystallized from hot water to give 0.19 g (0.83 mmol, 90% yield) of product **14** as the hydrochloride. ^{1}H NMR (D_2O): δ 3.10 (dd, 2H), 3.50 (dd, 2H), 6.64 (m, 2H), 7.02 (d 1H). MS (EI): 193 (M^+). A small portion of this product was neutralized with NaOH to yield the free base, **14**, as a white precipitate. Mp 264–266 °C (lit.[31] Mp 252–254 °C). The hydrochloride form of **14** (0.19 g, 0.83 mmol) was dissolved in 30 mL of dioxane/water (2:1) with Na_2CO_3 (0.9 g, 8.6 mmol) and di-*tert*-butyl dicarbonate (1.02 g, 4.7 mmol), and the solution was stirred at room temperature for 3 h. The solvent was then removed under vacuum, the residual oil was dissolved in 15 mL of cold water, the pH was adjusted to 3 with cold 1 N HCl, and the solution was extracted five times with cold ethyl acetate. The organic extracts were combined, dried over $MgSO_4$, and filtered. Solvent was removed under vacuum to afford 0.15 g (0.51 mmol, 61% yield) of the racemic N^{α}-*tert*-butyloxycarbonyl-

protected amino acid, Boc-Hai, **15**. ^{1}H NMR (CD_3OD): δ 6.9 (m, 1H, aromatic), 6.4 (m, 2H, aromatic), 3.5 (m, 2H, βCH_2), 3.3 (m, 2H, βCH_2), 1.4 (s, 9H, Boc). MS (CI): 294 (MH^+).

2-Amino-6-hydroxytetralin-2-carboxylic Acid Hydrobromide (Hat, 16).[32] A mixture of 6-methoxy-2-spiro[hydantointetralin] (3.6 g, 14.6 mmol), prepared from 6-methoxy-2-tetralone,[32] and aqueous 48% HBr (50 mL) was refluxed for 48 h. The aqueous HBr was evaporated, and the residue was dissolved in 150 mL of water; 4 g of charcoal was added, and the mixture was warmed on a steam bath and then filtered. After evaporation of the water, the residue was crystallized from ethanol to give 3.8 g of white powder in 90% yield. Mp 276–278 °C dec (lit.[32] mp 275 °C dec). ^{1}H NMR (DMSO-d_6): δ 9.21 (s, 1H, OH), 8.27 (s, 2H, NH_2), 6.91 (d, J = 7.97 Hz, 1H, aromatic), 6.55 (m, 2H, aromatic), 3.15 (d, J = 16.6 Hz, 1H, one of βCH_2), 2.74 (m, 3H, one of βCH_2 and $\beta' CH_2$), 2.10 (m, 1H, one of γCH_2), 1.93 (m, 1H, one of γCH_2). MS (CI): 208 (MH^+).

(+)- and (−)-2-[(*tert*-Butyloxycarbonyl)amino]-6-hydroxytetralin-2-carboxylic Acid [(+)-N$^\alpha$-Boc-Hat, 18, and (−)-N$^\alpha$-Boc-Hat, 19]. A stirred solution of **16** (2.5 g, 8.7 mmol) in 50 mL of methanol was cooled in an ice bath and then treated with thionyl chloride (3.4 g) added dropwise. After the addition was completed, the reaction mixture was stirred at room temperature for 14 h. The solvent was evaporated, and the residue was treated with 50 mL of 4 N ammonium hydroxide and extracted with 3 × 60 mL of ethyl acetate. The organic extracts were combined, dried over $MgSO_4$, filtered, and evaporated *in vacuo* to give 1.7 g of methyl 2-amino-6-hydroxytetralin-2-carboxylate, **17**, as an oil in 90% yield. ^{1}H NMR (DMSO-d_6): δ 8.98 (s, 1H, OH), 6.81 (d, J = 8.3 Hz, 1H, aromatic), 6.47 (m, 2H, aromatic), 3.60 (s, 3H, OCH_3), 2.97 (d, J = 16.3 Hz, 1H, βCH_2), 2.78 (m, 1H, $\beta' CH_2$), 2.57 (m, 2H, βCH_2 and $\beta' CH_2$), 1.92 (m, 1H, γCH_2), 1.75 (m, 1H, γCH_2). HRMS: calcd for $C_{12}H_{15}NO_3$, 221.1052; found, 221.1050.

The greater ability of the L-enantiomer of the methyl ester of Hat to serve as a substrate for chymotrypsin[35] was used to partially resolve the racemic amino acid. A mixture of **17** (1.7 g, 8.2 mmol), chymotrypsin (13.5 mg), ammonium bicarbonate (0.4 g), water (51 mL), and DMF (9 mL) was stirred at room temperature for 22 h and then concentrated. The resulting residue was dissolved in 50 mL of water and extracted with 3 × 50 mL of ethyl acetate. The aqueous layer, containing free amino acid, was reserved, and the organic layers were combined, dried over $MgSO_4$, filtered, and concentrated.

The residue from the organic layers was treated with chymotrypsin (14 mg), ammonium bicarbonate (0.2 g), water (20 mL), and DMF (6 mL), stirred at room temperature for 7 h, and then concentrated. The residue was dissolved in 30 mL of water, extracted with 3 × 30 mL of ethyl acetate, dried over $MgSO_4$, filtered, and evaporated *in vacuo*. The resulting residue was refluxed in 30 mL of aqueous 12 N HCl for 12 h and evaporated *in vacuo*. The resulting amino acid residue was checked by chiral TLC (silica gel RP modification coated with Cu^{2+} and chiral reagent; Art.-Nr. 811057, Mcherey-Nagel, Schweizerhall Inc.; elution solvent, acetonitrile/methanol/water, 15:4:1; R_f 0.49). The mixture of the residue in 30 mL of a dioxane/water (1:1) solution, di-*tert*-butyl dicarbonate (0.91 g, 4.2 mmol), and sodium carbonate (1.0 g) was stirred at room temperature for 24 h and then neutralized with citric acid (2 g) and concentrated. The residue was dissolved in 30 mL of water, extracted with 3 × 40 mL of ethyl acetate, dried over $MgSO_4$, filtered, and evaporated *in vacuo*. The residue was crystallized from dichloromethane to give 0.51 g of enantiomerically enriched (−)-N$^\alpha$-Boc-Hat (Boc-D-Hat), **18**, as a white powder in 20% yield. Mp 142–144 °C. $[\alpha]_D = -4.2°$ (c = 1.1, DMF) (lit.[35] $[\alpha]_D = 9.5°$). MS (CI): 308 (MH^+). ^{1}H NMR is consistent with the literature report for racemic N$^\alpha$-Boc-Hat.[11]

The aqueous layer containing free amino acid from above was concentrated and checked by chiral TLC (under the conditions mentioned above; R_f 0.56). The mixture of the residue in 30 mL of a dioxane/water (1:1) solution, di-*tert*-butyl dicarbonate (0.91 g, 4.2 mmol), and sodium carbonate (1.0 g) was stirred at room temperature for 24 h and then neutralized with citric acid (2 g) and concentrated. The residue was dissolved in 30 mL of water, extracted with 3 × 40 mL of ethyl acetate, dried over $MgSO_4$, filtered, and evaporated *in vacuo*. The residue was crystallized from dichloromethane to give 0.61 g of enantiomerically enriched (+)-N$^\alpha$-Boc-Hat (Boc-L-Hat), **19**, as a white powder in 24% yield. Mp 143–145 °C. $[\alpha]_D = +3.6°$ (c = 1.3, DMF) (lit.[35] $[\alpha]_D = +7.7°$). MS (CI): 308 (MH^+). ^{1}H NMR is consistent with the literature report for racemic N$^\alpha$-Boc-Hat.[11]

Diethyl 1-Acetyl-5-hydroxy-3-(4′-methoxyphenyl)pyrrolidine-2,2-dicarboxylate (20). In a manner similar to that of Cox et al.,[33] sodium (0.13 g, 5.7 mmol) was added to a solution of diethyl acetamidomalonate (12.2 g, 56.1 mmol) in ethanol (USP dehydrated, 200 proof, 75 mL) and stirred under N_2 until dissolved. The solution was chilled in an ice water bath; *p*-methoxycinnamaldehyde (10.0 g, 61.7 mmol) was added, and the solution was stirred for 2 h at room temperature. TLC indicated an incomplete reaction, so sodium (0.10 g, 4.3 mmol) was added, and the solution was stirred overnight. After 18 h, acetic acid was added to pH 4 and the solvents were removed *in vacuo* to leave a yellow viscous oil. The oil was dissolved in benzene (50 mL) and filtered, and petroleum ether (bp 30–65 °C, 50 mL) was slowly added. The oily residue was triturated to a solid and recrystallized from benzene/petroleum ether to give 14.9 g (70% yield) of a white crystalline solid. Mp 88.7–89.0 °C. TLC: R_f 0.14 (EtOAc/hexane, 2:1, UV visualization). EI MS: *m/e* 379 (M^+).

Diethyl 1-Acetyl-3-(4′-methoxyphenyl)pyrrolidine-2,2-)dicarboxylate (21). By the method of Chung et al.,[34] trifluoroacetic acid (9.5 mL) was added in a dropwise fashion to a stirred solution of **20** (4.70 g, 12.4 mmol) and triethylsilane (3.0 mL, 19 mmol) in $CHCl_3$ (25 mL) at room temperature. The solution was stirred for 4.5 h at room temperature, and the solvents were removed *in vacuo*. Ethyl acetate (80 mL) was used to dissolve the resultant transparent oil, and the solution was carefully washed with saturated $NaHCO_3$ (3 × 40 mL), NaCl (40 mL), and H_2O (40 mL). The ethyl acetate solution was dried over Na_2SO_4 and filtered, and the solvents were removed *in vacuo* to leave 4.58 g of the title product as a biphasic, milky oil which was used without further purification. TLC: R_f 0.24 (EtOAc/hexanes, 2:1, UV visualization). EI MS: *m/e* 363 (M^+).

***N*-Acetyl-3-(4′-methoxyphenyl)proline (22).** Following the procedure of Sarges and Tretter,[36] the diester **21** (14.9 g, 0.41 mmol) was dissolved in dioxane (distilled, 70 mL) and a solution of NaOH (4.92 g, 0.123 mol) in H_2O (17 mL) was added. The mixture was refluxed for 22 h, cooled, filtered, and partially rotary evaporated to remove dioxane. The basic aqueous solution was washed with EtOAc (2 × 50 mL) and carefully acidified to pH 2 with cold 3 N HCl. The solution was extracted with EtOAc (3 × 100 mL), and the organic layers were combined, dried over $MgSO_4$, and filtered and the solvents removed *in vacuo* to give 4.21 g (39% yield) of the title product as a gold oil containing all four stereoisomers which could be analytically resolved into *cis* and *trans* enantiomeric pairs by HPLC (see below). TLC: R_f 0.34 (1.5% AcOH/EtOAc, UV visualization); R_f 0.75 (EtOAc/AcOH/MeOH/H_2O, 70:10:20:5, UV and 2,6-dichlorophenol/indophenol visualization). HPLC (Vydac 218TP C-18 column, 0.46 cm × 25 cm; 0.1% (w/v) TFA in H_2O/0.1% TFA in CH_3CN using a 0–70% gradient of the organic component over 70 min at 1 mL/min, monitored at 280 nm): t_R 30.4 (33%), 31.5 min (52%). A small analytical sample of each peak was isolated by HPLC, and each gave EI MS *m/e* 263 (M^+), 218 ($M - CO_2$)$^+$.

***N*-(*tert*-Butyloxycarbonyl)-*trans*-3-(4′-hydroxyphenyl)proline (23) and *N*-(*tert*-Butyloxycarbonyl)-*cis*-3-(4′-hydroxyphenyl)proline (24).** *N*-Acetyl-3-(4′-methoxyphenyl)proline (**22**; 3.39 g, 12.9 mmol), as a mixture of all four stereoisomers, was dissolved in glacial AcOH (25 mL) and 6 N HCl (80 mL). The material was refluxed for 18 h, and the solvents were removed *in vacuo*. The residue was dissolved in H_2O (100 mL) and washed with EtOAc (2 × 50 mL). The aqueous layer was evaporated to dryness to give 2.99 g of a gray, crystalline solid which was dissolved in dioxane (40 mL) and H_2O (40 mL) and stirred at room temperature. Di-*tert*-butyl dicarbonate (6.19 g, 28.4 mmol) was added to the solution, and triethylamine was added dropwise to give pH 9. The mixture was stirred overnight at room temperature. The

solvents were removed *in vacuo*, and the residue was partitioned between cold H_2O (40 mL) and cold EtOAc (40 mL). Cold 1 M HCl was added dropwise with stirring to adjust the solution to pH 2. The layers were separated, and the aqueous layer was extracted with EtOAc (2 × 40 mL). The combined organic layers were washed with cold NaCl (2 × 25 mL) and cold H_2O (25 mL) and dried over $MgSO_4$. Filtration and removal of solvents *in vacuo* gave 2.61 g of a tan foam. TLC: R_f 0.52, 0.60 (0.5% AcOH/EtOAc, UV and 2,6-dichlorophenol/indophenol visualization). Analytical HPLC (Vydac 218TP C-18 column, 0.46 cm × 25 cm; 0.1% (w/v) TFA in H_2O/0.1% (w/v) TFA in CH_3CN using a 0–70% gradient of the organic component over 70 min at 1 mL/min, monitored at 280 nm) gave four major products with t_R 39.2 (22%), 40.8 (10%), 48.1 (14%), and 48.6 min (50%) with respective EI MS *m/e* 307 (M^+), 307 (M^+), 321 (M^+), and 321 (M^+). The latter two peaks were apparently the result of incomplete phenolic methyl ether deprotection. Flash chromatography of 2.6 g of crude material on 220 g of silica gel with elution by 0.5% (w/v) AcOH/EtOAc failed to give good resolution. *N*-(*tert*-butyloxycarbonyl)-*trans*-3-(4′-hydroxyphenyl)proline (**23**, Boc-*t*-Hpp) was cleanly separated from the *cis* isomer, Boc-*c*-Hpp (**24**), by semipreparative HPLC on a Vydac 218TP 2.2 cm × 25 cm C-18 column with the solvent system 0.1% (w/v) TFA in H_2O/0.1% TFA in CH_3CN using 28% of the organic component isocratically at 10 mL/min to yield 0.57 g (1.9 mmol) of **23** and 0.21 g (0.7 mmol) of **24**, a combined yield of 21%. The two isomers were distinguished on the basis of ^1H NMR spectral analysis[13] and assigned as *trans* isomer (peak 1, t_R 39.2 min) and *cis* isomer (peak 2, t_R 40.8 min).

Receptor Binding Assays. Receptor binding assays on guinea pig brain membrane homogenates were performed at 25 °C using a previously described protocol.[37] Binding affinities of test ligands for μ, δ, and κ opioid receptors were determined by competition with radiolabeled receptor selective ligands [^{3}H]DAMGO, [^{3}H]DPDPE, and [^{3}H]U69,593, respectively. For μ and δ receptor binding, IC_{50} values were obtained by linear regression from plots relating inhibition of specific binding to the log of 11 different ligand concentrations, using the computer program LIGAND[38] (Biosoft Software). K_i values were similarly calculated using values for K_D of each ligand, determined by analysis of saturation binding experiments. Values of K_D were determined for each membrane preparation used and were in the following ranges: K_D = 1.18–1.72 nM for [^{3}H]DPDPE; K_D = 1.06–2.68 nM for [^{3}H]DAMGO. For each analogue, K_i values reported in Table 1 represent the mean of two to four independent determinations, each performed in triplicate. For binding to κ receptors, expected to be weak for all analogues, the protocol was altered to include only five ligand concentrations (in duplicate). Analysis by LIGAND, using K_D = 1.04–2.25 nM for [^{3}H]U69,593, yielded estimates or lower limits for K_i.

GPI and MVD Bioassays. Electrically induced smooth muscle contractions of mouse vas deferens and strips of guinea pig ileum longitudinal muscle–myenteric plexus were used as bioassays.[39] Tissues from male ICR mice weighing 25–40 g or male Hartley guinea pigs weighing 250–500 g were tied to gold chain with suture silk, suspended in 20 mL baths containing 37 °C oxygenated (95% O_2, 5% CO_2) Krebs bicarbonate solution (magnesium free for MVD), and allowed to equilibrate for 15 min. The tissues were then stretched to optimal length, previously determined to be 1*g* tension (0.5*g* for MVD), and allowed to equilibrate for 15 min. The tissues were stimulated transmurally between platinum wire electrodes at 0.1 Hz, 0.4 ms pulses (2.0 ms pulses for MVD), and supramaximal voltage. The test peptides were added to the baths in 14–60 μL volumes. The agonists remained in contact with the tissue for 3 min before the addition of the next cumulative doses, until maximum inhibition was reached. Percent inhibition was calculated by using the average contraction height for 1 min preceding the addition of the agonist divided by the contraction height 3 min after exposure of the agonist. IC_{50} values represent the mean of two to four tissues. IC_{50} estimates and their associated standard errors were determined by fitting the mean data to the Hill equation using a computerized nonlinear least squares method (PCNOCIN and NONLIN84, Statistical Consultants Inc.).

Computational Studies. Molecular mechanic calculations for **1** and its analogues were done in two stages as previously described.[7] First, the set of low-energy conformers of the common cyclic fragment CH_3CO-c[D-Cys-Ala-D-Pen]OH was calculated. Second, these conformers of the cyclic fragment were combined with conformers of the modified first residue and the Phe^3 side chain and minimized again.

In the first stage of the computations, all possible combinations of backbone torsion angles φ and ψ within the cycle CH_3-CO-c[D-Cys-Ala-D-Pen]OH (with a step of 30° within sterically allowed regions of the Ramachandran plot) and the rotamers of D-Cys^2 and D-Pen^4 side chains (χ^1 = ±60° and 180°) were generated and minimized initially with the ECEPP/2 force field[40] using the program CONFORNMR.[41] "Soft" parabolic disulfide bond-closing functions $U(r - r)^2$ were used with ECEPP/2 (U = 30 kcal/mol Å^2 for S–S bond and C^β–S–S valence angles) since it was observed that the use of the usual closing functions (U = 100 kcal/mol Å^2) within the small conformationally strained cycle of **1** led to an apparent increase of relative energy for some conformers which was inconsistent with results obtained with the CHARMm force field. Low-energy conformers identified in this fashion (ΔE < 10 kcal/mol) in which at least one torsion angle differed by >30° were selected and minimized additionally with the QUANTA 3.3/CHARMm force field.[42] All possible side chain conformations of *t*-Hpp, *c*-Hpp, Hai, Hat, D-Hat, and HO-Tic methylamides (Table 4) were calculated with CHARMm.

In the second stage of computations, the low-energy conformers of the fragment CH_3CO-c[D-Cys-Ala-D-Pen]OH (ΔE < 4 kcal/mol with CHARMm) were combined with conformers of the Phe^3 side chain and the first residue (including combinations of sterically allowed values for the first residue ψ and D-Cys^2 φ torsion angles with a 50° step) and minimized again with the CHARMm force field. For all calculations, a compromise value of dielectric constant, ϵ = 10, was used and the adopted basis Newton–Raphson method of minimization was employed. This intermediate value of ϵ has previously been found to be appropriate for the conformational analysis of peptides[43] and for computations of electrostatic energy in proteins.[44] The QUANTA 3.3 Molecular Similarity system was used for all superpositions.

Acknowledgment. This work was supported by the National Institute on Drug Abuse through Grant DA03910 and Grant DA00118 (Research Scientist Development Award) to H.I.M. Financial support for D.L.H. was provided by The American Foundation for Pharmaceutical Education, The National Institutes of Health (Training Grant GM07767), and The Horace H. Rackham School of Graduate Studies at The University of Michigan. H.B.K. is grateful for support from a National Institute on Drug Abuse Institutional National Research Service Award, DA07268. We thank Peg Davis for performing the GPI and MVD assays.

References

(1) Rizo, J.; Gierasch, L. Constrained Peptides: Models of Bioactive Peptide and Protein Substructures. *Annu. Rev. Biochem.* **1992**, *61*, 387–418.
(2) Hruby, V. J. Conformational and Topographical Considerations in the Design of Biologically Active Peptides. *Biopolymers* **1993**, *33*, 1073–1082.
(3) Mosberg, H. I.; Hurst, R.; Hruby, V. J.; Gee, K.; Yamamura, H. I.; Galligan, J. J.; Burks, T. F. Bis-Penicillamine Enkephalins Possess Highly Improved Specificity Toward Delta Opioid Receptors. *Proc. Natl. Acad. Sci. U.S.A.* **1983**, *80*, 5871–5874.
(4) Mosberg, H. I.; Omnaas, J. R.; Medzihradsky, F.; Smith, C. B. Cyclic, Disulfide- and Dithioether-Containing Opioid Tetrapeptides: Development of a Ligand with High Delta Opioid Receptor Selectivity and Affinity. *Life Sci.* **1988**, *43*, 1013–1020.
(5) Schiller, P. W.; Maziak, L. A. Synthesis and Activity Profiles of Novel Cyclic Opioid Peptide Monomers and Dimers. *J. Med. Chem.* **1985**, *28*, 1766–1771.

(6) Pelton, J. T.; Kazmierski, W.; Gulya, K.; Yamamura, H. I.; Hruby, V. J. Design and Synthesis of Conformationally constrained Somatostatin Analogues with High Potency and Specificity for Mu Opioid Receptors. *J. Med. Chem.* **1986**, *29*, 2370–2375.

(7) Lomize, A.; Flippen-Anderson, J.; George, C.; Mosberg, H. Conformational Analysis of the δ Receptor-Selective, Cyclic Opioid Peptide, Tyr-*cyclo*[D-Cys-Phe-D-Pen]OH (JOM-13). Comparison of X-ray Crystallographic Structures, Molecular Mechanics Simulations, and ^{1}H NMR Data. *J. Am. Chem. Soc.* **1994**, *116*, 429–436.

(8) Kazmierski, W.; Wire, S. W.; Lui, G. K.; Knapp, R. J.; Shook, J. E.; Burks, T. F.; Yamamura, H. I.; Hruby, V. J. Design and Synthesis of Somatostatin Analogues with Topographical Properties that Lead to Highly Potent and Specific μ Opioid Receptor Antagonists with Greatly Reduced Binding at Somatostatin Receptors. *J. Med. Chem.* **1988**, *31*, 249–253.

(9) Schiller, P. W.; Weltrowska, G.; Nguyen, T. M.-D.; Lemieux, C.; Chung, N. N.; Marsden, B. J.; Wilkes, B. C. Conformational Restriction of the Phenylalanine Residue in a Cyclic Opioid Peptide Analogue: Effects on Receptor Selectivity and Stereospecificity. *J. Med. Chem.* **1991**, *34*, 3125–3132.

(10) Tourwe, D.; Toth, G.; Lebl, M.; Verschueren, K.; Knapp, R. J.; Davis, P.; Van Binst, G.; Yamamura, H. I.; Burks, T. F.; Kramer, T.; Hruby, V. J. A Simple Synthesis of 1,2,3,4,-tetrahydro-7-hydroxyisoquinoline-3-carboxylic acid (HO-Tic) a Conformationally Restricted Tyrosine Analogue and its Incorporation into Opioid Peptides. In *Peptides Chemistry and Biology, Proceedings of the Twelfth American Peptide Symposium*; Smith, J. A., Rivier, J. E., Eds.; ESCOM: Leiden, 1992; pp 307–308.

(11) Deeks, T.; Crooks, P. A.; Waigh, R. D. Synthesis and Analgesic Properties of Two Leucine-Enkephalin Analogues Containing a Conformationally Restrained N-Terminal Tyrosine Residue. *J. Med. Chem.* **1983**, *26*, 762–765.

(12) Toth, G.; Russell, K. C.; Landis, G.; Kramer, T.; Fang, L. G.; Knapp, R. J.; Davis, P.; Burks, T. F.; Yamamura, H. I.; Hruby, V. J. Ring Substituted and Other Conformationally Constrained Tyrosine Analogues of [D-Pen^2, D-Pen^5]Enkephalin with δ Opioid Receptor Selectivity. *J. Med. Chem.* **1992**, *35*, 2384–2391.

(13) Mosberg, H. I.; Kroona, H. B. Incorporation of a Novel Conformationally Restricted Tyrosine Analogue into a Cyclic, δ Opioid Receptor Selective Tetrapeptide (JOM-13) Enhances Delta Receptor Binding Affinity and Selectivity. *J. Med. Chem.* **1992**, *35*, 4498–4500.

(14) Paton, W. D. M. The Action of Morphine and Related Substances on Contraction and Acetylcholine Output of Coaxially Stimulated Guinea Pig Ileum. *Br. J. Pharmacol.* **1957**, *12*, 119–127.

(15) Henderson, G.; Hughes, J.; Kosterlitz, H. W. A New Example of a Morphine Sensitive Neuroeffector Junction. *Br. J. Pharmacol.* **1972**, *46*, 764–766.

(16) Shimohigashi, Y.; Costa, T.; Pfeiffer, A.; Herz, A.; Kimura, H.; Stammer, C. Cyclopropyl ^{E}Phe^4-enkephalin Analogs. Delta Receptors in Rat Brain are Different from Those in Mouse Vas Deferens. *FEBS Lett.* **1987**, *222*, 71–74.

(17) Tourwe, D.; Meert, D.; Couder, J.; Ceusters, M.; Elseviers, M.; van Binst, G.; Toth, G.; Burks, T. F.; Schook, J. E.; Yamamura, H. I. Synthesis and Biological Activities of Linear and Cyclic Enkephalin Analogs Containing a Gly$^3\psi$(E, CH=CH)Phe^4 Replacement. In *Peptides: Chemistry, Structure, and Biology, Proceedings of the 11th American Peptide Symposium*; Rivier, J. E., Marshall, G. R., Eds.; ESCOM: Leiden, 1990; pp 331–333.

(18) Jiang, Q.; Takemori, A. E.; Sultana, M.; Portoghese, P. S.; Bowen, W. D.; Mosberg, H. I.; Porreca, F. Differential Antagonism of Opioid Delta Antinociception by [D-Ala^2, Leu^5, Cys^6]Enkephalin (DALCE) and Naltrindole 5'-isothiocyanate (NTII): Evidence for Delta Receptor Subtypes. *J. Pharmacol. Exp. Ther.* **1991**, *257*, 1069–1075.

(19) Mattia, A.; Vanderah, T.; Mosberg, H. I.; Porreca, F. Lack of Antinociceptive Cross Tolerance Between [D-Pen^2, D-Pen^5]-Enkephalin and [D-Ala^2]Deltorphin II in Mice: Evidence for Delta Receptor Subtypes. *J. Pharmacol. Exp. Ther.* **1991**, *258*, 583–587.

(20) Sofuoglu, M.; Portoghese, P. S.; Takemori, A. E. Differential Antagonism of *Delta* Opioid Agonists by Naltrindole and Its Benzofuran Analogue (NTB) in Mice: Evidence for *Delta* Opioid Receptor Subtypes. *J. Pharmacol. Exp. Ther.* **1991**, *257*, 676–680.

(21) Watson, G.; Lanthorn, T. Electrophysiological Actions of Delta Opioids in CA1 of the Rat Hippocampal Slice are Mediated by One Delta Receptor Subtype. *Brain Res.* **1993**, *601*, 129–135.

(22) Stewart, P. E.; Hammond, D. L. Evidence for Delta Opioid Receptor Subtypes in Rat Spinal Cord-Studies with Intrathecal Naltriben, Cyclic[D-Pen^2, D-Pen^5] Enkephalin and [D-Ala^2, Glu^4]-Deltorphin. *J. Pharmacol. Exp. Ther.* **1993**, *266*, 820–828.

(23) Wild, K. D.; Carlisi, V. J.; Mosberg, H. I.; Bowen, W. D.; Portoghese, P. S.; Sultana, M.; Takemori, A. E.; Hruby, V. J.; Porreca, F. Evidence for a Single Functional Opioid Delta Receptor Subtype in the Mouse Isolated *Vas Deferens*. *J. Pharmacol. Exp. Ther.* **1993**, *264*, 831–838.

(24) DeGrado, W. F. Design of Peptides and Proteins. *Adv. Protein Chem.* **1988**, *39*, 51–124.

(25) Hruby, V.; Gehrig, C. Recent Developments in the Design of Receptor Specific Opioid Peptides. *Med. Res. Rev.* **1989**, *9*, 343–401.

(26) Mosberg, H. I.; Porreca, F. A Model for the Structural Basis of δ_2-Opioid Receptor Selectivity. In *Medications Development: Drug Discovery, Databases, and Computer-Aided Drug Design*; Rapaka, R., Hawks, R., Eds.; NIDA Research Monograph 134; National Institute on Drug Abuse: Rockville, MD; 1993; pp 268–280.

(27) Dohlman, H. G.; Thorner, J.; Caron, M. G.; Lefkowitz, R. J. Model Systems for the Study of Seven-Transmembrane-Segment Receptors. *Annu. Rev. Biochem.* **1991**, *60*, 653–688.

(28) Nikiforovich, G. V.; Hruby, V. J.; Prakash, O.; Gehrig, C. A. *Biopolymers* **1991**, *31*, 941–955.

(29) Heath, W. F.; Tam, J. P.; Merrifield, R. B. Improved Deprotection of Cysteine-Containing Peptides in HF. *Int. J. Pep. Protein Res.* **1986**, *28*, 498–507.

(30) Ellman, G. L. Tissue Sulfhydryl Groups. *Arch. Biochem. Biophys.* **1959**, *82*, 70–77.

(31) Pinder, R.; Butcher, B.; Buxton, D.; Howells, D. 2-Aminoindan-2-carboxylic Acids: Potential Tyrosine Hydroxylase Inhibitors. *J. Med. Chem.* **1971**, *14*, 892–893.

(32) Rastogi, S. N.; Bindra, J.; Anand, N. α-Methyldopa in a Rigid Framework: 3-Amino-3-methyl-6,7-dihydroxy-3,4-dihydrocoumarins & 2-Amino-6,7-dihydroxytetralin-2-carboxylic Acids. *Indian J. Chem.* **1971**, *9*, 1175–1182.

(33) Cox, D. A.; Johnson, A. W.; Mauger, A. B. A Modified Proline Synthesis. *J. Chem. Soc.* **1964**, 5024–5029.

(34) Chung, J. L.; Wasicak, J.; Arnold, W.; May, C.; Nadzan, A.; Holladay, M. Conformationally Constrained Amino Acids. Synthesis and Optical Resolution of 3-Substituted Proline Derivatives. *J. Org. Chem.* **1990**, *55* 270–275.

(35) Cardinaux, F.; Pless, J. Morphine-like Structures and Semi-Rigid Sidechains as Molecular Probes for the Bioactive Conformation of Enkephalin. In *Peptides 1984. Proceedings of the 18th European Peptide Symposium*; Ragnarsson, U., Ed.; Almqvist & Wiksell International: Stockholm, Sweden; 1984; pp 321–324.

(36) Sarges, R.; Tretter, J. Synthesis of Aryl-Substituted 1,3- and 1,4-Diazocine Derivatives. *J. Org. Chem.* **1974**, *39*, 1710–1716.

(37) Heyl, D. L.; Mosberg, H. I. Substitution on the Phe^3 Aromatic Ring in Cyclic δ Receptor-Selective Dermorphin/Deltorphin Tetrapeptide Analogues: Electronic and Lipophilic Requirements for Receptor Affinity. *J. Med. Chem.* **1992**, *35*, 1535–1541.

(38) Munson, P. J.; Rodbard, D. LIGAND: A Versatile Computerized Approach for Characterization of Ligand-Binding Systems. *Anal. Biochem.* **1980**, *107*, 220–239.

(39) Shook, J.; Pelton, J.; Wire, W.; Hirning, L.; Hruby, V.; Burks, T. Pharmacologic Evaluation of a Cyclic Somatostatin Analogue with Antagonist Activity at *Mu* Opioid Receptors *in Vitro*. *J. Pharmacol. Exp. Ther.* **1987**, *240*, 772–777.

(40) Momany, F. A.; McGuire, R. F.; Burgess, A. W.; Scheraga, H. A. Energy Parameters in Polypeptides. VII. Geometric parameters, Partial Atomic Charges, Nonbonded Interactions, Hydrogen Bond Interactions, and Intrinsic Torsional Potentials for the Naturally Occuring Amino Acids *J. Phys. Chem.* **1975**, *79*, 2361–2381.

(41) Lomize, A. L.; Pervushin, K. V.; Arseniev, A. S. Spatial Structure of (34–65)bacterioopsin Polypeptide in SDS Micelles Determined from Nuclear Magnetic Resonance Data. *J. Biomol. NMR* **1992**, *2*, 361–372.

(42) Momany, F. A.; Rone, R. Validation of the General Purpose QUANTA 3.2/CHARMm Force Field. *J. Comput. Chem.* **1992**, *13*, 888–900.

(43) Lipkind, G. M.; Arkhipova, S. F.; Popov, E. M. Theoretical Conformational Analysis of Methylamides of N-acetyl-L-serine and N-acetyl-L-asparagine. *Int. J. Pept. Protein Res.* **1973**, *5*, 381–397.

(44) Warshel, A.; Aqvist, J. Electrostatic Energy and Macromolecular Function. *Annu. Rev. Biophys. Biophys. Chem.* **1991**, *20*, 267–298.